https://doi.org/10.3311/PPee.36820

Periodica Polytechnica Electrical Engineering and Computer Science

A Self-adapting Pixel Antenna - Substrate Lens System for Infrared Frequencies

Mustafa Shubbar[1*], Balázs Rakos[1]

[1] Department of Automation and Applied Informatics, Faculty of Electrical Engineering and Informatics, Budapest University of Technology and Economics, Műegyetem rkp. 3., H-1111 Budapest, Hungary
[*] Corresponding author, e-mail: shubbar@aut.bme.hu

Received: 07 March 2024, Accepted: 31 May 2024, Published online: 01 July 2024

Abstract

In this work, we propose a concentrator lens - antenna arrangement, potentially suitable for infrared sensing and energy harvesting rectenna systems. The structure consists of a pixel antenna, self-adapting for the direction of the incident infrared radiation, and a concentrator lens, both optimized for the mid-infrared spectrum. The silicon substrate lens is situated above the pixel antenna, enabling the concentration of the incident light on the antenna; silicon was chosen due to its transparency in the IR spectrum. We examine how various parameters of the lens, in conjunction with the different states of the pixel antenna, affects the performance of the system. The simulations show that the gain of the arrangement increases considerably in correlation with the radius of the lens. The results suggest that the energy conversion efficiency of infrared rectenna systems can be enhanced by several orders of magnitude with the utilization of the proposed arrangement.

Keywords

substrate lens, infrared antenna, pixel antenna, rectenna, infrared sensor, infrared energy harvesting, MOM diode

1 Introduction

1.1 Rectenna-based Infrared detectors

Recently, there has been a significant surge in the utilization of infrared detectors regarding various fields such as medicine, telecommunication, space science, energy harvesting and military [1–3]. Generally, the sensors can be grouped as follows: photon detectors exploit the photonic nature of the incident light by utilizing the quantum-mechanical effect that emerges in semiconductors. Conversely, the operation of thermal detectors is based on the temperature elevation of the material due to the absorbed radiation, which changes their resistance, like in the case of bolometers or thermocouple detectors. The output signal does not depend on the photonic nature of the incident radiation [4]. The third type of detectors is the wave detector, that operates by taking advantage of the electromagnetic nature of the radiation. Generally, such detectors are composed of an antenna and a rectifier (rectenna). The incident electromagnetic radiation generates a high-frequency current within the antenna, coupled to a nonlinear rectifying element. This system can produce a direct current at the output [5, 6].

The development of IR detectors faces various difficulties, mainly related to the longer wavelength-end of the spectrum (e.g., mid-IR range). These challenges are concerned with the spectral response, cooling requirements, cut-off frequency, responsivity, and size. Rectenna system-based sensors present a promising solution for such limitations. Furthermore, the antenna in such arrangements offers excellent frequency response and spatial domain control, and permits the realization of spatially compact sensors and large collection area. These capabilities are not inherently available in conventional IR sensors. Such integrated devices can also operate at ambient temperature [7].

Gou et al. [8] suggest that the utilization of spiral antenna yields significantly enhanced tunable absorption of the microbridge structure operating at THz frequencies. This approach leads to the fabrication of THz frequency microbolometer detectors with promising capabilities in real-time imaging applications. Bonakdar et al. [9] demonstrate the enhancement of light-matter interactions in quantum wells and boost the responsivity of these detectors by applying optical antenna. In their study, Florence et al. [10] employ a V-shaped, linear tapered slot antenna (V-LTSA), effectively coupled to a metal-oxide-metal (MOM) diode, operating at 10.6 μm wavelength.

Cite this article as: Shubbar, M., Rakos, B. "A Self-adapting Pixel Antenna - Substrate Lens System for Infrared Frequencies", Periodica Polytechnica Electrical Engineering and Computer Science, 2024. https://doi.org/10.3311/PPee.36820

Due to its promising characteristics, this particular sensor is expected to become highly demanded for broadband IR detection. Morf et al. [11] introduce a novel sensor concept that relies on an antenna, coupled to MOSFET bolometers, which can operate at ambient temperatures. A broad-bandwidth THz antenna that effectively absorbs the electromagnetic field is directly coupled to the bolometer to optimize the collected energy. Additionally, this design reduces the thermal mass, a critical factor for fast frame rate in security and medical applications.

1.2 Rectenna-based energy harvesting systems

The demand for electric power has increased dramatically in the last few decades. Although fossil fuel-based power generation is predominant, it contributes to environmental pollution by billions of tons of carbon dioxide emission. Therefore, there is considerable interest in alternative, environment-friendly energy sources.

Solar radiation is a dominant source of clean energy, since the power density of 1370 W/m^2 reaches the earth's surface. The solar spectrum consists of infrared (IR), visible light, and ultraviolet (UV) radiation with 52%, 39%, and 9%, respectively [12, 13]. Additionally, heat can emit infrared radiation with a wavelength between 8–14 μm [12, 14]. Utilizing this type of renewable energy has opened a new era for producing clean electricity [12]. The utilization of photovoltaics-based technology has continuously increased since its first application in 1950. Although semiconductor-based photovoltaics (PV) provides a convenient method for directly converting sunlight into electricity, it has many drawbacks, like its low energy conversion efficiency, the high cost of materials, and the difficulty of the fabrication process. Furthermore, they cannot utilize the mid-IR range of the solar spectrum, the most considerable portion of solar energy. Sensitivity to weather conditions, and rapidly deteriorating efficiency with increasing temperature are also shortcomings of such technology. Moreover, the application of mechanical sun-tracking systems is necessary to achieve maximum conversion efficiency [12, 15, 16].

The application of nanoantenna has gained much interest regarding solar and IR energy harvesting systems, since it can be a potential alternative to traditional solar energy harvesting methods [15, 17]. Antenna-based structures offer distinct advantages, since they are widely available in various forms and can be manufactured using inexpensive and simple fabrication processes compared to conventional solar cells. Furthermore, they can achieve significantly higher efficiency than solar cells and utilize the environmental IR radiation available 24 hours a day, such as heat [11, 15].

Jayaswal et al. [18] and Sabaawi et al. [12] presented a novel bowtie antenna for IR field capture along with the proposed metal-insulator-metal (MIM) diode for rectifying high-frequency currents. Other studies demonstrate an alternative rectification process to address the mismatching problem. In their work, Szakmany et al. [19] and González et al. [20] proposed a concept of antenna integrated together with thermoelectric junctions. The electric current is produced by the Seebeck effect due to heating of the hot junction by the received IR radiation. In contrast, Chekin et al. [21] proposed nanoantenna placed in an array to achieve a high electric field. The aforementioned study suggests a different rectification process related to electron field emission from sharp edges in a vacuum, based on the Fowler-Northeim (FN) theory.

Similarly to other types of electromagnetic waves, infrared radiation can be detected and captured by an antenna. This concept of using antenna for solar energy harvesting purposes was first introduced in 1972 by Bailey [22]. The electromagnetic radiation can be harvested by rectifying the current induced in the antenna by utilizing a high-speed rectifier (rectenna system) [11, 23, 24]. The block diagram of the arrangement is displayed in Fig. 1. The system's total efficiency depends on the efficiency of each part, and their matching level [23]. Consequently, many researchers focused on antenna gain, matching level, and rectification process. Citroni et al. [24] demonstrated a dynamic impedance matching between an optical rectenna array and the load. This technique aims to maximize the captured power and improve the conversion efficiency by addressing the crucial mismatching problem.

Since antennas with high gain and directivity are essential for medical sensing and energy harvesting applications, implementing reconfigurable antenna in these systems could be an excellent solution [25]. Poorgholam-Khanjari et al. [26] employed graphene slabs to obtain reconfigurable properties that improve the antenna return

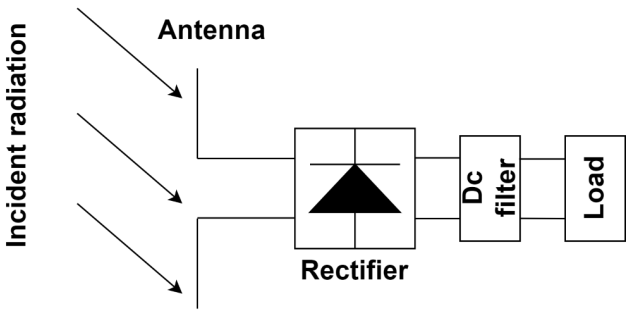

Fig. 1 Block diagram of the energy harvesting system based on the rectenna principle

loss and its bandwidth. Zarrabi et al. [27] incorporated a graphene coating on the cross-shaped nano-aperture to achieve reconfigurable characteristics of the antenna. Furthermore, Bazgir et al. [28] improved the characteristics of nanoantenna by applying a unique metamaterial, and their reconfiguration is achieved by using a graphene layer coating. Shubbar and Rakos [29] offer an IR pixel antenna structure that enables the antenna pattern to be dynamically adjusted towards the direction of the incident radiation. This reconfigurability results in a considerable enhancement of the antenna gain.

1.3 Application of substrate lenses for performance enhancement

Unfortunately, there are some limitations regarding the utilization of antenna in the terahertz band: the path loss increases to a considerable level and the directivity of the antenna becomes lower. Therefore, many researchers focused on magnifying the captured energy for solar cells and antenna with the aid of optical devices like trapping systems and lenses. Applications of substrate lens antenna have been used to overcome these drawbacks as an example of this technology. Tvingstedt et al. [30] presented light absorption enhancement with 25% increase in photocurrent by evolving an innovative light trapping system based on an array of microlenses. Jha et al. [31] demonstrate a groundbreaking structure containing a ring resonator microstrip antenna integrated into a hemi-elliptical lens at terahertz frequencies. The study shows that the overall directivity of any system can be improved by the utilization of a dielectric lens; specifically, they found that using a silicon substrate lens improved the directivity by 11.52 dBi. Yasuoka et al. [32] examine the performance of the double-slot antenna operating at 700 GHz. The antenna was integrated with a hemispherical lens with a radius of 7.3 mm. The results of the investigation indicated a considerable enhancement in the detected sensitivity with an increase of 31.4 dB.

The concentration factor of the lens can be determined by the utilization of idealized models of spherical and cylindrical lenses, along with the application of Snell's law of refraction. This allows for assessing the light-focusing scenario, where an ideal lens directs sunlight towards its focal point. The flux of the light that traverses the lens can be expressed as follows [14]:

$$TS_1A_1 = S_2A_2 \tag{1}$$

Where the lens area is , the image area is , the incident solar irradiance is , and the captured solar irradiance is . By taking the transmittance factor of the silicon lens, T, as unity at terahertz frequencies and replacing the area with the radius

$$S_2 = 2S_1\frac{R^2}{r_{img}^2}, \tag{2}$$

where R and r_{img} are the radius of the lens (hemispherical) and captured image (circle), respectively.

1.4 Antenna-coupled MOM diode

Metal-Oxide-Metal (MOM) diodes, also commonly called Metal-Insulator-Metal (MIM), are composed of an insulator sandwiched by two parallel metallic layers. When these two layers consist of the same material, the diode is symmetrical; if the electrodes are made from different materials, the diode is asymmetrical [6]. Generally, the required insulator thickness is less than 4 nm to allow electron tunneling through the insulator. Since the tunneling mechanism is nonlinear, and very fast (on the order of femtosecond), the diode exhibits rectifying properties at infrared frequencies [6, 33].

The antenna-coupled MOM diode system can be characterized by the circuit diagram displayed in Fig. 2 [6]. The antenna operates at the resonance frequency and can be modeled by a high-frequency voltage source with V_0 amplitude, an antenna resistance, R_a, and an antenna reactance, X_a. The antenna parameters depend on the antenna geometry, material, and substrate properties, they can be determined with the aid of an electromagnetic simulator software.

MOM diodes can be described by a nonlinear resistance, R_d in parallel with a capacitance, C_d, which can be described by [6].

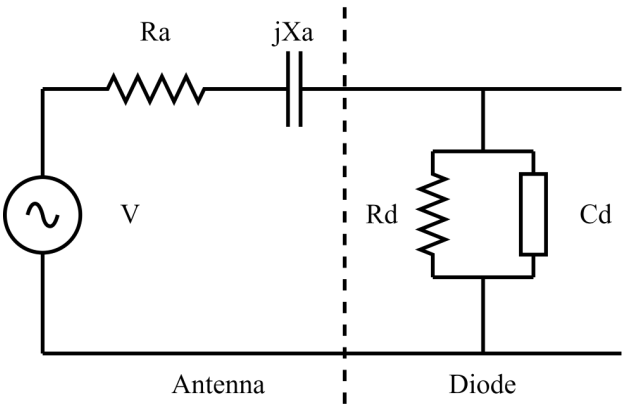

Fig. 2 Equivalent circuit diagram of an antenna-coupled MOM diode

$$C_d = \varepsilon_{ox}\varepsilon_o \frac{A}{D}, \tag{3}$$

where ε_{ox} is the relative permittivity of the oxide in the MOM diode, while ε_o is the permittivity of free space, A refers to the junction area, and D represents the thickness of the insulator. The dielectric constant of Al_2O_3 at a frequency of 28.3 THz is approximately 1. Since the antenna resistance is normally on the order of 100 ohms in the case of mid-IR frequencies, the junction capacitance must be less than 0.1fF. This can be achieved by fabricating the contact area of the diode very small [14]. The diode capacitance with a 25 Å barrier thickness and 50 × 50 nm overlap area equals 8.85E-19 Farad [6].

The rectification process of MOM diodes is based on nonlinear electron tunneling [6] through the oxide barrier of the junction, which results in a DC current. The rectified signal is then directly related to the nonlinearity of the current-voltage curve, commonly referred to as the curvature coefficient (γ) of the diode, and the amplitude of the rectified signal can be determined by [6]:

$$I_r = 2\gamma \frac{R_d R_a A_{em} S}{\left(R_a + R_d - C_d \omega X_a R_d\right)^2 + \left(X_a + R_a R_d \omega C_d\right)^2}. \tag{4}$$

Where S is the irradiance of the radiation, and A_{em} is the maximum effective area of the antenna, which can be calculated by [34].

$$A_{em} = \frac{G\lambda^2}{4\pi} \tag{5}$$

Where G is the gain of the antenna.

2 Self-adapting infrared pixel antenna

Conventional wireless systems usually possess predefined objectives. Therefore, the antenna in these systems have predefined characteristics regarding both the frequency and spatial domains [25, 35]. In the past few years, reconfigurable antennas have had a significant surge in research interest regarding multi-stander applications and scenarios that require continuous optimization of the antenna performance [35, 36]. Antennas can be made self-adapting by altering their physical or electrical parameters with the aid of internal mechanisms to redistribute the RF currents in them [37]. Pixel antenna is one of the most attractive ideas for the realization of reconfigurable antennas [38, 39]. The operational principle of such structures is similar to that of an LCD screen, as both can realize arbitrary shapes [40]. Pixel antennas typically comprise a two-dimensional grid of small metallic surfaces (patches), interconnected by sub-wavelength dimension switches.

The self-adjusting pixel antenna used in this study has been introduced in [29, 41]. It consists of 3 × 3 square pixels, as depicted in Fig. 3(b). These pixels are constructed by interconnected square patches using small metallic parts functioning as switches. Each square pixel in the given system has a side length of 1.5 μm, the spacing between adjacent patches is 0.2 μm, and the dimensions of the metallic connectors are 0.4 μm × 0.2 μm. The square pixels are placed on a SiO_2 layer supported by an intrinsic silicon substrate with a thickness of 600 μm and a relative permittivity of ϵ_r = 11.9. The optimized thickness of the SiO_2 layer is 0.8 μm, and its relative permittivity is ϵ_r = 3.9 [29, 42]. In [29], we simulated the antenna structure using the Sonnet professional software. Since Sonnet is incapable of simulating the lens structure, in this work we used the Ansys HFSS software, which can simulate concentrator lens structures. In this investigation the supporting silicon layer was eliminated in order to simplify and accelerate the simulation process. We found that such simplification didn't affect the results.

Bolometers with well-designed geometry can be made sensitive for radiation incident from specific directions. The application of such bolometers as switches between neighboring pixels allows for the realization of a self-adjusting antenna that can optimize its characteristics based on the angle of incidence of the radiation (as mentioned in [29, 41]). Several materials with various temperature coefficients of resistance (TCR) have the potential to be used as a bolometer, such as nickel, niobium, and vanadium oxide. They can even be made sensitive to specific directions, like the nickel bolometers reported in [43]. The proposed design is optimized to be sensitive to the incident radiation only from specific directions, mainly perpendicular, west, north, and east. The necessary directionalities of the switches are summarized in Table 1.

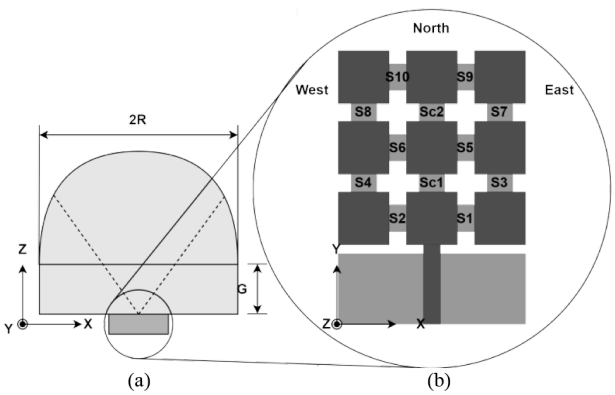

Fig. 3 Substrate lens (a)-pixel antenna geometry with the bolometer switches (b) used for the simulations

Table 1 Directionalities of the bolometers in the pixel antenna structure

Arrangement 1	
Switch	Directionality
S5, S6, S7, S8, S9, S10, Sc2	perpendicular
S2, S4	perpendicular and west
S1, S3	perpendicular and east
Sc1	perpendicular and north
Arrangement 2	
Switch	Directionality
S5, S6, S9, S10	perpendicular
S2, S4, S8	perpendicular and east
S1, S3, S7	perpendicular and west
Sc1, Sc2	perpendicular and north

Multiple configurations of switches can be utilized to accomplish the task; here, we present two solutions. When the radiation is of perpendicular incidence, all of the bolometers switch to their ON state, resulting in all of the pixels being connected. In the case of radiation coming from the northward direction, the center switch, Sc1 will be in its ON state, or both Sc1 and Sc2 in the other configuration; therefore, the radiation pattern of the antenna will lean toward the north. On the other hand, if the IR radiation hits from the west, S1, and S3, or, in the case of the other configuration, S1, S3, and S7 will be activated, tilting the radiation pattern westward. The similar consideration applies when the IR radiation arrives from the eastward direction. In this scenario, the S2 and S4, or in the other arrangement, S2, S4, and S8, will result in an eastward shift of the radiation pattern [29, 41].

In the following, we present simulation results regarding the gain enhancement of a system consisting of the afore-described self-adapting pixel antenna coupled to microlenses, designed for the mid-IR range.

3 Simulation of the pixel antenna - hemispherical dielectric lens system

The power density of the solar irradiance on the rectenna can be increased by the utilization of solar concentrators. The energy conversion efficiency of these systems can be theoretically enhanced with the aid of spherical and cylindrical polymer microlenses. These microlenses can direct solar radiation toward their focal point, where rectennas can be positioned. This technology aims to improve solar energy conversion efficiency by increasing light trapping [44].

Our proposed system is based on a reconfigurable pixel antenna presented in [29] in combination with a substrate lens and a MOM diode rectifier. The application of a properly designed lens considerably improves the gain of the arrangement. This will be demonstrated in the following sections through simulations with the Ansys HFSS 2021 software, backed by mathematical calculations based on theoretical models.

This section investigates the effects of a substrate lens on the pixel antenna performance. Fig. 3(a) illustrates the lens structure utilized in this study, which comprises a convex lens with a radius R, and a cylindrical section with a height of G. Since the lens must be transparent for THz frequencies, its material is assumed to be silicon.

3.1 All of the pixels are connected

The initial gain of the antenna without lens when all of the switches are in their ON state is 3.57 dB with an aperture efficiency of 81.4%. Simulation results demonstrate that adding a lens with an initial radius of $R = 5$ μm assuming that all of the switches are in the ON state, results in a gain enhancement of 3.5 dB. In this study, we investigate the effects of the parameters of the lens on the pixel antenna performance. Fig. 4 shows the radiation pattern of the antenna-lens arrangement when all of the switches are turned to the ON state. The pattern clearly indicates that the radiation pattern of the system is directed to the perpendicular direction.

Fig. 5 shows the calculated and simulated antenna gain when a concentrator lens is placed over the antenna. It demonstrates a linear relationship between the antenna gain and lens radius. The obtained outcomes are consistent with Eq. (2), which shows that the collected power is proportional to R^2. The relationship appears linear when the data is plotted on a logarithmic scale (dB). However, Fig. 5 shows that the calculated gain is higher than the simulated results when using a larger lens. This discrepancy is due to the losses of the lens. Absorption, reflection, and dispersion losses may effectively reduce the efficiency of the lens [44, 45].

Additionally, the data presented in Fig. 6 reveals a direct relationship between the gap, G between the antenna and the lens, where a larger lens necessitates a greater gap to achieve the maximum gain at the antenna. The result aligns with theoretical expectations, since, from the lens-maker's formula, the focal length is

$$f = \frac{1}{n-1} \times \frac{1}{R}, \tag{6}$$

where n is the refractive index of the lens, which is equal to 3.5 at mid-IR wavelengths.

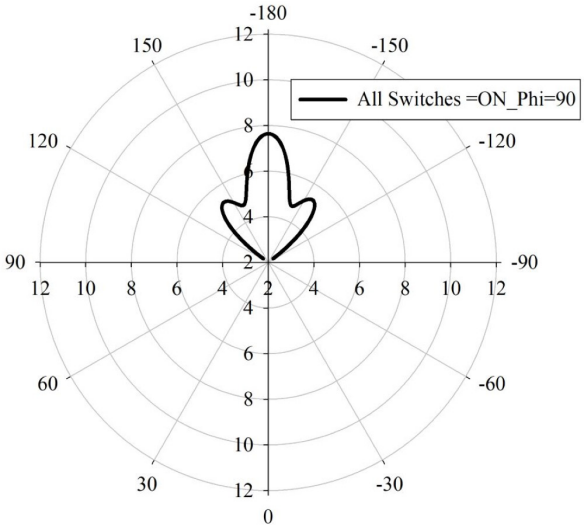

(a)

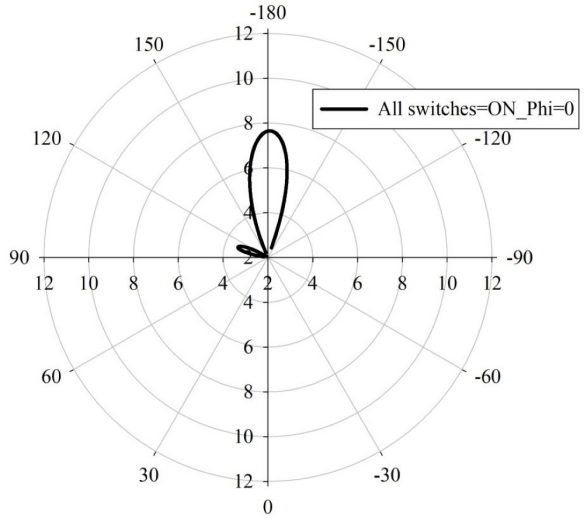

(b)

Fig. 4 E-plane (xz-plane) (a) and H-plane (yz-plane) (b) radiation patterns when all of the switches are turned to the ON state and $R = 10$ µm

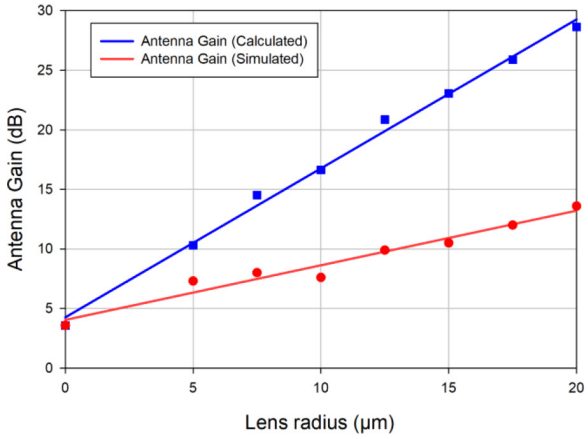

Fig. 5 Antenna gain versus lens radius when all switches are ON

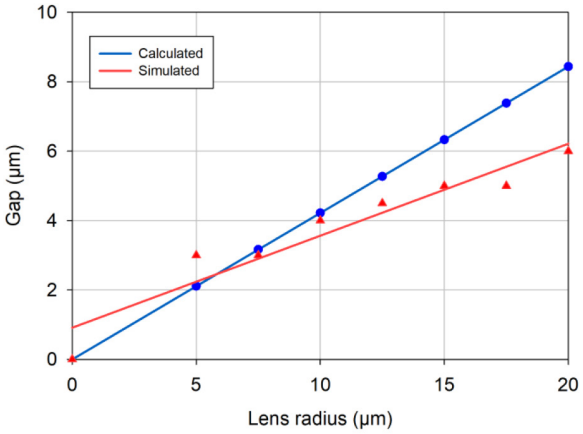

Fig. 6 Optimal gap (filled by silicon) for different lens radiuses when all of the switches are ON

3.2 Center pixels are connected

When the incoming radiation arrives from the northward direction, the switch Sc1 is set to its ON state in "arrangement 1". Alternatively, in the case of "arrangement 2", the switches Sc1 and Sc2 are set to ON as described in Table 1. All of the other switches are assumed to be in their OFF state. The current distribution of the states are along the y-axis when the center switches Sc1 and Sc2 are activated. This change in current distribution results in a radiation pattern tilted northwards (please refer to [29]).

Fig. 7(b) shows that the H-plane radiation pattern of the antenna is directed northward in the case when Sc1 = ON and Sc1 = Sc2 = ON. This demonstrates that the application of the concentrator lens preserves the directionality of the antenna (see Table 2). Moreover, a considerable improvement of the antenna gain is observed (see Fig. 8), with a linear dependence on the radius of the lens. The antenna gain in the absence of the concentrator lens when Sc1 = ON and Sc1 = Sc2 = ON are 3.2 dB and 3.9 dB, respectively. The aperture efficiency of the antenna in the aforementioned cases is 74% and 88%, respectively. However, the system's gain increases by more than double when a lens with a 5 µm radius is applied. In alternative terms, the system exhibits an about 3 dB increase in gain for every 5 µm increment in lens radius.

Additionally, a slightly smaller gap is required in the case of the present arrangement than in the previous case (all switches are ON). This is due to the fact that the lens must be slightly off-focus, as the pixels in the ON state are located outside the focal point.

3.3 Side pixels are connected

Configuring the antenna into symmetrical patterns resembling mirror images leads to mirroring the current

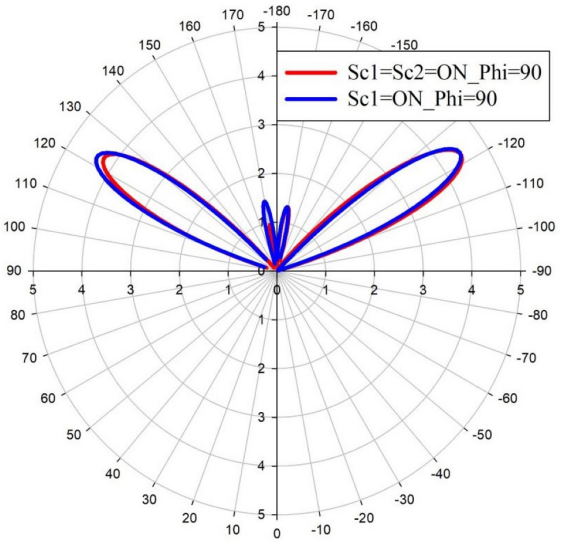

(a)

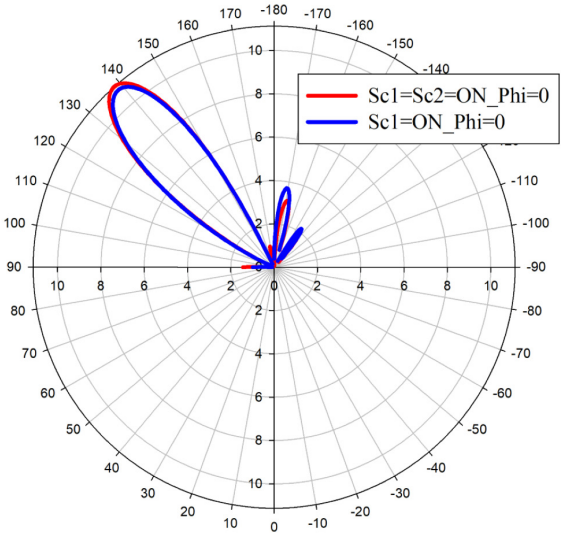

(b)

Fig. 7 *E*-plane (xz-plane) (a) and *H*-plane (yz-plane) (b) radiation patterns when Sc1 = On and Sc1 = Sc2 = ON and R = 10 μm

Table 2 Characteristics of the substrate lens - pixel antenna system in the case of incoming IR radiation at various angles of incidence

Direction of incidence	Antenna configuration	Maximum Gain G_0 (dB)	Effective area A_{em} (μm²)
Isotropic	Dipole antenna	2.1	14.5
Isotropic	Pixel antenna with all switches ON	3.57	20.3
Perpendicular	Pixel antenna, Sc1 = ON	3.2	18.7
Perpendicular	Pixel antenna, Sc1 = Sc2 = ON	3.94	22.15
West and east	Pixel S1 = S3 = ON and S2 = S4 = ON	3.3	19.11
Perpendicular	Substrate lens (R = 15μm) ALL switches ON	10.5	100.3
Perpendicular	Substrate lens (R = 15 μm) Pixel antenna, SC1 = ON	14.2	235.2
Perpendicular	Substrate lens (R = 15 μm) Pixel antenna, SC1 = SC2 = ON	13.8	214.5
West and east	Substrate lens (R = 15 μm) Pixel S1 = S3 = ON and S2 = S4 = ON	14.3	240.7

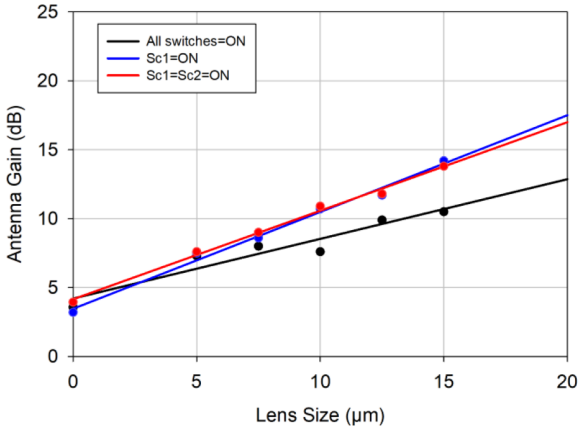

Fig. 8 Antenna gain versus lens radius in the case of Sc1 = ON state, Sc1 = Sc2 = ON state, and all switches are in ON state

distribution across the pixels. Since the physical lengths remain identical, the frequency responses are identical in these two cases: S1 = S3 = ON (this occurs when radiation is incident from the east as per Table 1) and S2 = S4 = ON state (radiation is from the west per Table 1), while all of the other switches are in the OFF state. The radiation patterns of these two states are mirror images; when S1 = S3 = ON, the radiation pattern leans towards the east, and when S2 = S4 = ON, the antenna pattern is westward-directed. The mirrored current distributions explain this behavior. A comprehensive simulation and explanation were published in [29].

Fig. 9(a) demonstrates that the E-plane patterns are mirror images of each other. When both S1 and S3 are set to ON, the radiation pattern tilts eastward, and when both S2 and S4 are set to ON, the antenna pattern points westward, while Fig. 9(b) displays the identical H-plane patterns. The behavior is explained by the mirrored current distributions.

Fig. 10 displays the gain of the system versus the radius of the lens. If S1 = S3 = ON, or S2 = S4 = ON, the antenna gain in the absence of the concentrator lens is 3.3 dB and the aperture efficiency is 76%. However, there is a linear gain improvement of the system when a concentrator lens

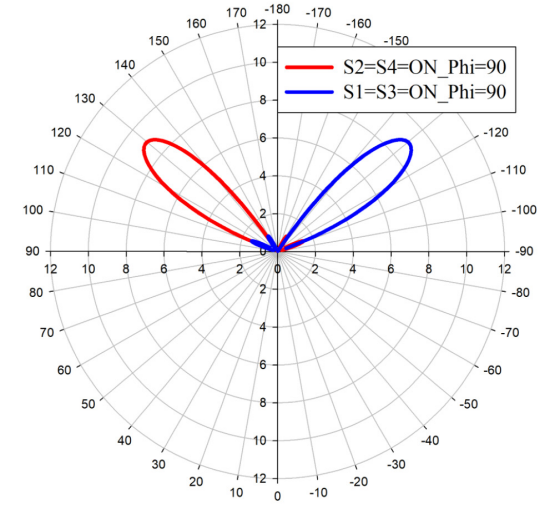

(a)

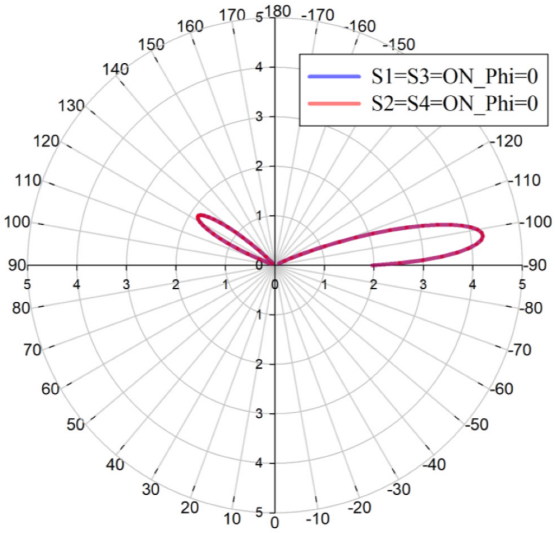

(b)

Fig. 9 *E*-plane (xz-plane) (a) and *H*-plane (yz-plane) (b) radiation patterns when S1 = S3 = ON and S2 = S4 = ON and R = 10 μm

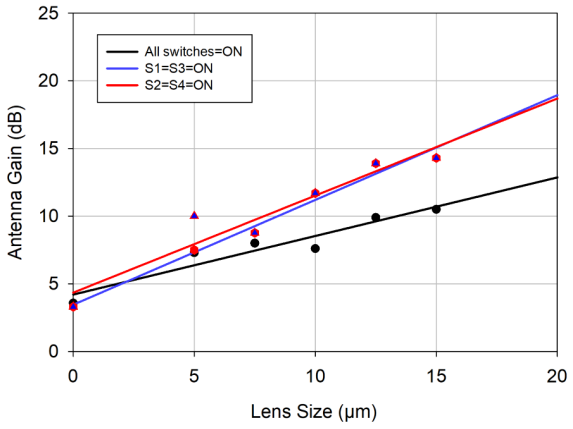

Fig. 10 Antenna gain versus lens radius in the case of S1 = S3 = ON state, S2 = S4 = ON state, and all of the switches are in ON state

with increasing radius is used. The trend is similar to that discussed in the previous section; a 5 μm lens radius has the potential to enhance the antenna gain by 3.2 dB. On average, the system exhibits an approximate 3 dB increase in gain with every 5 μm increase in lens radius.

4 Concentrator lens - pixel antenna - MOM diode system

As we described it in the introduction, various potential rectifiers exist that may be integrated together with our proposed substrate lens - antenna system in order to realize infrared sensing or energy harvesting devices. In this section, we utilize the data of a MOM diode rectifier, used in a MOM diode - dipole antenna IR rectenna system, described in [5], to demonstrate the theoretically expected performance improvements provided by our arrangement.

In [5] the length of the dipole antenna was 3.1 μm, designed for the 28.3 THz radiation. The MOM diode had an approximately 50 × 50 nm contact area with a 25 Å barrier thickness. Since the relative dielectric constant of Al_2O_3 at 28.3 THz is approximately 1, the diode capacitance is C_d = 8.85E-19 F. The zero bias resistance of the diode, R_d = 220 kΩ, and the average zero bias curvature of the diode, γ = 0.74 V^{-1} [5]. For the calculations, we used the circuit model described in [6], characterized by equations 3–5. To ensure the validity of the model, we simulated the design presented in [5] in a previous work [46]. The result shows that both the simulated and measured rectified currents are close to each other, and both reflect the linear characteristics of the detector in response to the incident power.

The simulated antenna characteristics of the different antenna arrangments are summarized in Table 2, Fig. 11 shows the rectenna responses. The results illustrate that the rectified current of the pixel antenna (without using a

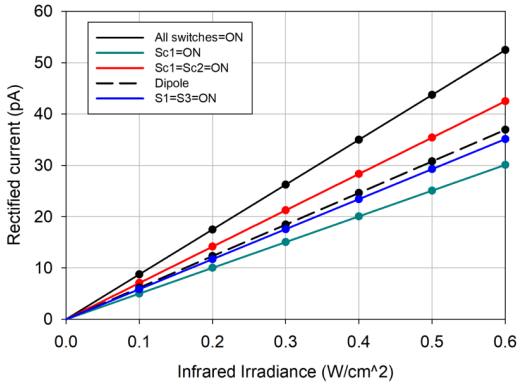

Fig. 11 Rectified current versus irradiance in the case of different antenna arrangements, in the absence of lens

concentrator lens) is higher than that in the case of the proposed dipole antenna - MOM diode device in literature, when all of the switches are in the ON state, and when Sc1 = Sc2 = ON by 43% and 17%, respectively. The incorporation of a concentrator lens into the system improves the performance even more. Fig. 12 displays the rectified current at the output of the concentrator lens - pixel antenna - MOM diode system in the case of the different antenna configurations. The rectified current obtained from the proposed arrangement exhibits a significantly greater value than that achieved in [5]. For instance, when all of the switches are in the ON state, with S1 and S3 being ON, Sc1, and Sc2 being ON, and Sc1 being ON, the rectified current values are 7.8, 13, 20, and 21 times respectively.

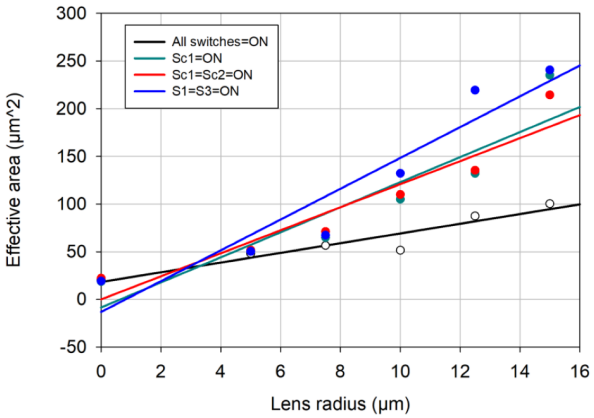

Fig. 13 Effective area of the concentrator lens - antenna system versus lens radius

5 Discussion

The simulation results show that the proposed pixel antenna - concentrator lens system possesses promising characteristics, it is potentially suitable for high-gain, mid-IR sensor and energy harvesting applications. The concentrator lens significantly increases the effective area of the arrangement. Fig. 13 shows that the effective area can be increased by around five times when a lens with a 15 μm radius is applied in conjunction with the antenna, when all of the pixels are interconnected. On the other hand, the effective area of the system is increased by more ten times in other antenna states (see Fig. 13), suggesting that the directive gain of the system is increased in the case of these configurations, as well, when a concetrator lens is applied. The substrate lens concentrates the collected energy to the focal spot, where the antenna is situated, hence, the lens can maximize the power density. The simulations show that the gain of the pixel antenna - concentrator lens structure increases linearly with the radius

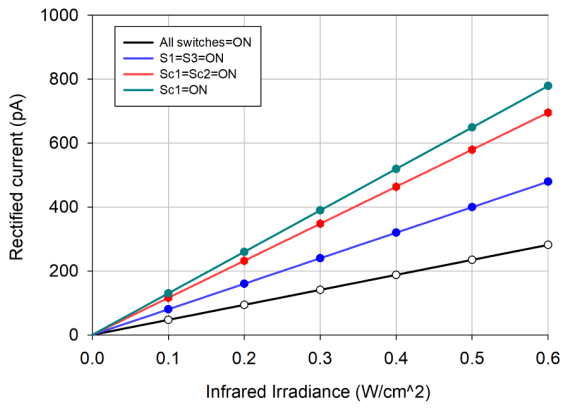

Fig. 12 Rectified current versus irradiance in the case of the lens - pixel antenna - MOM diode system when R = 10 μm

of the lens. The observations are in accordance with theory.The directional sensitivity of the self-adapting pixel antenna in the lens - antenna system is clearly observable, since the gain of the different antenna configurations sensitive to certain directions is much higher (average 3 dB) than the gain when all of the pixels are interconnected. The validity of the linear relationship between lens radius and collected power depends on various factors. Larger lenses may introduce aberrations and distort the wavefront, reducing power collection efficiency. Absorption in the material, and path length increase with larger lens diameter, potentially lead to increased losses.

Various elementary electronic devices exist that can be utilized as rectifiers for infrared frequency currents, such as the Seebeck effect [20], electron field emission from sharp edges in vacuum, based on Fowler-Nordheim (FN) theory [21], and MOM diodes based on electron tunneling. In this study, we chose the well-tested MOM diode for demonstrating the performance enhancement of our proposed lens - pixel antenna system. The investigation shows that the proposed pixel antenna improves the rectified current by the MOM diode by 42% compared to the dipole system. Moreover, the application of the substrate lens over the pixel antenna structure can increase the rectified current by 5 times to 25 times, (please refer to Fig. 11 and Fig. 12). This increase is expected to grow monotonically as the lens is made even larger.

The performance of the proposed system may be improved further by reducing losses concerning reflections and absorption. Fabrication and actual testing of the system is also of paramount importance. Various fabrication techniques can be used for practical implementation. These methods can be categorized into direct and indirect

methods, based on their working principles. Direct methods eliminate the need for fabricating a mask or mold insert with concave 3D microstructures. Some examples of direct methods include hot embossing, inkjet printing, electrohydrodynamic jet printing, thermal reflow of photoresist, laser-based fabrication methods, and self-assembly. On the other hand, indirect methods, such as wet etching and soft lithography, are commonly employed for microlens fabrication.

6 Conclusion

We examined the impact of a silicon substrate lens on the self-adapting, mid-IR pixel antenna that was introduced in our previous study. The simulations demonstrate that the utilization of the concentrator lens significantly increases the gain, thereby the effective area of the system, while preserving the directionality of the radiation pattern of the antenna. The enhancement is twofold, when a lens with a 5 μm radius is applied, and the increase of the gain exhibits a nearly linear correlation with the radius. The results are in accordance with expectations based on lens theory. Our proposed arrangement can be integrated together with a high-speed rectifier element, such as a metal-insulator-metal diode, in order to realize a rectenna system-based infrared sensor or energy harvesting device. Since substrate microlenses can be fabricated by applying various, readily available fabrication processes, we think, that the implementation of our system is possible with contemporary technology.

References

[1] Mubarak, M., Sidek, O., Abdel-Rahman, M. Mustaffa, M., Mustapa Kamal, A., Mukras, S. "Nano-Antenna Coupled Infrared Detector Design", Sensors, 18(11), 3714, 2018. https://doi.org/10.3390/s18113714

[2] Goh, N. W.-J., Poh, J.-J., Yeo, J.-Y., Aw, B. J.-J., Lai, S. C., Cheng, J. J. W., Tan, C. Y. L., Gan, S. K.-E. "Design and Development of a Low Cost, Non-Contact Infrared Thermometer with Range Compensation", Sensors, 21(11), 3817, 2021. https://doi.org/10.3390/s21113817

[3] Mancilla, R. B., Tấn, B. P., Daul, C., Martínez, J. G., Salas, L. L., Wolf, D., Hernández, A. V. "Anatomical 3D Modeling Using IR Sensors and Radiometric Processing Based on Structure from Motion: Towards a Tool for the Diabetic Foot Diagnosis", Sensors, 21(11), 3918, 2021. https://doi.org/10.3390/s21113918

[4] Rogalski, A. "Recent progress in infrared detector technologies", Infrared Physics & Technology, 54(3), pp. 136–154, 2011. https://doi.org/10.1016/j.infrared.2010.12.003

[5] Bean, J. A., Tiwari, B., Bernstein, G. H., Fay, P., Porod, W. "Thermal infrared detection using dipole antenna-coupled metal-oxide-metal diodes", Journal of Vacuum Science & Technology B, 27(1), pp. 11–14, 2009. https://doi.org/10.1116/1.3039684

[6] Rakos, B. "Investigation of Metal-oxide-metal Structures for Optical Sensor Applications", (Dissertation), University Of Notre Dame, 2006. [online] Available: https://curate.nd.edu/show/c247dr29087 [Accessed: 21 April 2022]

[7] Alda, J., Boreman, G. D. "Infrared antennas and resonant structures", SPIE Press, 2017. ISBN 9781510613584 [online] Available: https://spie.org/Publications/Book/2282290 [Accessed: 21 April 2022]

[8] Gou, J., Zhang, T., Wang, J., Jiang, Y. "Spiral Antenna-Coupled Microbridge Structures for THz Application", Nanoscale Research Letters, 12(1), 91, 2017. https://doi.org/10.1186/s11671-017-1857-7

[9] Bonakdar, A., Mohseni, H. "Impact of optical antenna and plasmonics on infrared imagers", Infrared Physics & Technology, 59, pp. 142–145, 2013. https://doi.org/10.1016/j.infrared.2012.12.029

[10] Florence, L. A., Slovick, B. A., Kinzel, E. C., Bean, J. A., Boreman, G. D. "Infrared Linear Tapered Slot Antenna", IEEE Antennas and Wireless Propagation Letters, 10, pp. 1299–1301, 2011. https://doi.org/10.1109/LAWP.2011.2176904

[11] Morf, T., Klein, B., Despont, M., Drechsler, U. Kull, L., Corcos, D., Elad, D. Kaminski, N., Pfeiffer, U. R., Hadi, R. A., ... Plettemeier, D. "Wide bandwidth room-temperature THz imaging array based on antenna-coupled MOSFET bolometer", Sensors and Actuators A: Physical, 215, pp. 96–104, 2014. https://doi.org/10.1016/j.sna.2014.03.019

[12] Sabaawi, A. M. A., Tsimenidis, C. C., Sharif, B. S. "Bow-tie nano-array rectenna: Design and optimization", In: 6th European Conference on Antennas and Propagation (EUCAP), Prague, Czech Republic, 2012, pp. 1975–1978. ISBN 9781457709180 https://doi.org/10.1109/EuCAP.2012.6206439

[13] Varsha, V. K.,Bhavana, S. J. "Terahertz antenna design for infrared energy harvesting applications", In: 2015 Radio and Antenna Days of the Indian Ocean (RADIO), Belle Mare, Mauritius, 2015, pp. 1–2. ISBN 9781467366908 https://doi.org/10.1109/RADIO.2015.7323390

[14] Kashif, M. F., Rakos, B. "A Nanoantenna-MIM Diode-Lens Device Concept for Infrared Energy Harvesting", In: Laukaitis, G. (ed.) Recent Advances in Technology Research and Education, Springer, 2019, pp. 169–176. ISBN 978-3319998336 https://doi.org/10.1007/978-3-319-99834-3_23

[15] Khoshdel, V., Joodaki, M., Shokooh-Saremi, M. "UV and IR cut-off filters based on plasmonic crossed-shaped nano-antennas for solar cell applications", Optics Communications, 433, pp. 275–282, 2019. https://doi.org/10.1016/j.optcom.2018.10.005

[16] Sabaawi, A. M. A., Al-Ani, O. A. "Solar Rectennas: Analysis and Design", In: Pinho, P. (ed.) Recent Wireless Power Transfer Technologies, IntechOpen, 2020. https://doi.org/10.5772/intechopen.89216

[17] Horikawa, J., Kawakami, A., Hyodo, M., Tanaka, S., Takeda, M., Shimakage, H. "Evaluation of nano-slot antenna for mid-infrared detectors", Infrared Physics & Technology, 67, pp. 21–24, 2014. https://doi.org/10.1016/j.infrared.2014.07.001

[18] Jayaswal, G., Belkadi, A., Meredov, A., Pelz, B. Moddel, G., Shamim, A. "Optical rectification through an Al_2O_3 based MIM passive rectenna at 28.3 THz", Materials Today Energy, 7, pp. 1–9, 2018. https://doi.org/10.1016/j.mtener.2017.11.002

[19] Szakmany, G. P., Orlov, A. O., Bernstein, G. H., Porod, W. "Nanoantenna arrays for infrared detection with single-metal nanothermocouples", Infrared Physics & Technology, 82, pp. 44–49, 2017. https://doi.org/10.1016/j.infrared.2017.02.008

[20] González, F. J., Dhakal, N., Boykin, T., Méndez-Lozoya, J., Peale, R. E. "Infrared pixel based on Seebeck nanoantennas", MRS Advances, 5(35), pp. 1837–1842, 2020. https://doi.org/10.1557/adv.2019.471

[21] Chekini, A., Sheikhaei, S., Neshat, M. "Nanoantenna arrays as diode-less rectifiers for energy harvesting in mid-infrared band", Microwave and Optical Technology Letterst, 61(2), pp. 412–416, 2019. https://doi.org/10.1002/mop.31562

[22] Bailey, R. L. "A Proposed New Concept for a Solar-Energy Converter," Journal of Engineering for Power, 94(2), pp. 73–77, 1972. https://doi.org/10.1115/1.3445660

[23] Ma Z., Vandenbosch, G. A. E. "Optimal solar energy harvesting efficiency of nano-rectenna systems", Solar Energy, 88, pp. 163–174, 2013. https://doi.org/10.1016/j.solener.2012.11.023

[24] Citroni, R., Di Paolo, F., Livreri, P. "Evaluation of an optical energy harvester for SHM application", AEU - International Journal of Electronics and Communications, 111, 152918, 2019. https://doi.org/10.1016/j.aeue.2019.152918

[25] Aboualalaa, M., Mohamed, H. A., Alghamdi, T. A. H., Alathbah, M. "A Pattern Reconfigurable Antenna Using Eight-Dipole Configuration for Energy Harvesting Applications", Sensors, 23(20), 8451, 2023. https://doi.org/10.3390/s23208451

[26] Poorgholam-Khanjari S., Zarrabi, F. B. "Reconfigurable Vivaldi THz antenna based on graphene load as hyperbolic metamaterial for skin cancer spectroscopy", Optics Communications, 480, 126482, 2021. https://doi.org/10.1016/j.optcom.2020.126482

[27] Zarrabi, F. B., Naser-Moghadasi, M., Heydari, S., Maleki, M., Arezomand, A. S. "Cross-slot nano-antenna with graphene coat for bio-sensing application", Optics Communications, 371, pp. 34–39, 2016. https://doi.org/10.1016/j.optcom.2016.03.048

[28] Bazgir, M., Naser-Moghadasi, M., Zarrabi, F. B., Arezomand, A. S., Heydari, S. "Nano particle implementation in nano loop antenna for energy harvesting application and light trapping", Optik, 132, pp. 127–133, 2017. https://doi.org/10.1016/j.ijleo.2016.12.033

[29] Shubbar M., Rakos, B. "A Self-Adapting, Pixelized Planar Antenna Design for Infrared Frequencies", Sensors, 22(10), 3680, 2022. https://doi.org/10.3390/s22103680

[30] Tvingstedt, K., Dal Zilio, S., Inganäs, O., Tormen, M. "Trapping light with micro lenses in thin film organic photovoltaic cells", Optics Express, 16(26), pp. 21608–21615, 2008. https://doi.org/10.1364/OE.16.021608

[31] Jha, K. R., Singh, G. "Ring-Resonator Integrated Hemi-Elliptical Lens Antenna at Terahertz Frequency", In: 2011 International Conference on Communication Systems and Network Technologies, Katra, Jammu, India, 2011, pp. 236–241. ISBN 9781457705434 https://doi.org/10.1109/CSNT.2011.58

[32] Yasuoka, Y., Suzuki, K., Abe, Y. "Fabrication of dielectric lens supported, antenna coupled, warm-carrier devices", Microelectronic Engineering, 73–74, pp. 496–501, 2004. https://doi.org/10.1016/S0167-9317(04)00200-X

[33] Briones, E., Alda, J., González, F. J. "Conversion efficiency of broad-band rectennas for solar energy harvesting applications", Optics Express, 21(S3), A412–A418, 2013. https://doi.org/10.1364/OE.21.00A412

[34] Balanis, C. A. "Antenna Theory: Analysis and Design", John Wiley & Sons, 2015. ISBN 978-1-118-642060-1

[35] Haider, N., Caratelli, D., Yarovoy, A. G. "Recent Developments in Reconfigurable and Multiband Antenna Technology", International Journal of Antennas and Propagation, 2013(1), 869170, 2013. https://doi.org/10.1155/2013/869170

[36] Li, P. K., Shao, Z. H., Wang, Q., Cheng, Y. J. "Frequency- and Pattern-Reconfigurable Antenna for Multistandard Wireless Applications", IEEE Antennas and Wireless Propagation Letters, 14, pp. 333–336, 2015. https://doi.org/10.1109/LAWP.2014.2359196

[37] George, R., Kumar, C. R. S., Gangal, S. A. "Design of a frequency reconfigurable pixel patch antenna for cognitive radio applications", In: 2016 International Conference on Communication and Signal Processing (ICCSP), Melmaruvathur, Tamilnadu, India, 2016, pp. 1684–1688. ISBN 9781467385497 https://doi.org/10.1109/ICCSP.2016.7754451

[38] Rodrigo, D., Cetiner, B. A., Jofre, L. "Frequency, Radiation Pattern and Polarization Reconfigurable Antenna Using a Parasitic Pixel Layer", IEEE Transactions on Antennas and Propagation, 62(6), pp. 3422–3427, 2014. https://doi.org/10.1109/TAP.2014.2314464

[39] Rodrigo D., Jofre, L. "Frequency and Radiation Pattern Reconfigurability of a Multi-Size Pixel Antenna", IEEE Transactions on Antennas and Propagation, 60(5), pp. 2219–2225, 2012. https://doi.org/10.1109/TAP.2012.2189739

[40] Kovitz J., Rahmat-Samii, Y. "Micro-actuated pixel patch antenna design using particle swarm optimization", In: 2011 IEEE International Symposium on Antennas and Propagation (APSURSI), Spokane, WA, USA, 2011, pp. 2415–2418. ISBN 9781424495627 https://doi.org/10.1109/APS.2011.5997009

[41] Shubbar M., Rakos, B. "An Angle-Sensitive, Nickel Bolometer-Based, Adaptive Infrared Pixel Antenna", In: Khakhomov, S., Semchenko, I., Demidenko, O., Kovalenko, D. (eds.) Research and Education: Traditions and Innovations, INTER-ACADEMIA 2021, , 2022, pp. 83–88. [online] Available at: https://link.springer.com/chapter/10.1007/978-981-19-0379-3_9 [Accessed: 21 April 2022]

[42] Shubbar, M. Rakos, B. "A Pixelized Infrared Antenna Design", In: Proceedings of the Automation and Applied Computer Science Workshop 2021 (AACS'21), Budapest, Hungary, 2021, pp. 60–68. ISBN 9789634218524

[43] Mohammadi, E., Behzadnezhad, B., Behdad, N. "An Angle-Sensing Infrared Detector Using a Two-Element Biomimetic Antenna Array", IEEE Transactions on Antennas and Propagation, 66(11), pp. 5818–5826, 2018. https://doi.org/10.1109/TAP.2018.2863112

[44] Tang, Z., Tress, W., Inganäs, O. "Light trapping in thin film organic solar cells", Materials Today, 17(8), pp. 389–396, 2014. https://doi.org/10.1016/j.mattod.2014.05.008

[45] Ribaudo, T., Passmore, B., Freitas, K., Shaner, E. A., Cederberg, J. G., Wasserman, D. "Loss mechanisms in mid-infrared extraordinary optical transmission gratings", Optics Express, 17(2), p. 666–675, 2009.
https://doi.org/10.1364/OE.17.000666

[46] Shubbar M., Rakos, B. "Performance Estimation of a Self-adapting Pixel Antenna-MOM Diode Infrared Energy Harvesting Device", In: Proceedings of the Automation and Applied Computer Science Workshop 2022 (AACS'22), Budapest, Hungary, 2022, pp. 213–221. ISBN 9789634218753